Short-term Prediction of Flow Rate and Suspended Sediment Transport in a Tidal River Using Genetic Programming

Chaiyuth Chinnarasri[1*], Pakorn Ditthakit[2]

[1]Water Resources Engineering and Management Research Center (WAREE), King Mongkut's University of Technology Thonburi (KMUTT), Bangkok 10140, Thailand
[2]School of Engineering and Resources Management, Walailak University, Nakhon Si Thammarat 80160, Thailand
* Corresponding author. Email: Chaiyuth.chi@kmutt.ac.th

ABSTRACT

Predicting flow rate and sediment transport are essential for water transportation, water resources management and drainage systems in lowland areas. This paper aims to develop simple models for predicting flow rate and suspended sediment transport in the lower Chao Phraya River, which has complicated flow characteristics. The predicted flow rate equations were developed based on genetic programming (GP) and the relationships among flow rates, water levels and flow directions during spring and neap tide periods. The prediction results for the short term show accurate performance with correlation coefficient (r) values greater than 0.88 for the training and testing processes (with the flow rates of -3,000 m^3/s to +3,000 m^3/s). The flow rate and nearshore sediment transport rate using the GP model in spring tide show more accuracy than those in the neap tide. During spring tide, there is a change in the water level that had a great influence on both the flow rate and the flow velocity. The flow direction is one of the important parameters for the proposed GP model that can be used for practical engineering applications for predicting flow rate and nearshore sediment transport rate for water management in the tidal river.

Keywords: Artificial intelligence, Flow characteristics, Genetic programming, Modelling, Suspended sediment transport.

Received 15-10-2022
Revised 19-12-2022
Accepted 23-12-2022

Notation List

A = cross-sectional area (m^2)
MAE = mean absolute error
n = manning's roughness coefficient ($s/m^{1/3}$)
N = number of observations
Q = discharge (m^3/s)
Q_f = discharge of non-uniform flow (m^3/s)
Q_0 = discharge of uniform flow (m^3/s)
q_s = nearshore sediment transport rate ($g/m^2/s$)
r = correlation coefficient
R = hydraulic radius of the river section (m)
RMSE = root mean square error
S_f = friction slope (dimensionless)
S_0 = bed slope or bottom slope (dimensionless)
S_w = water surface slope (dimensionless)
V_{max} = maximum velocity (m/s)
V_{mean} = mean velocity (m/s)
WL = water level (m, mean sea level)
X_i^{obs} = observed data
X_i^{pre} = predicted result
X_{mean}^{obs} = mean observed value
X_{mean}^{pre} = mean predicted value
y = flow depth (m)

1. INTRODUCTION

Tides can be described as phenomena resulting from gravitational attractions among the Sun, the Moon and Earth. These attractions of the gravitational forces differ depending on the Moon's and the Sun's positions relative to that of Earth. If they are on the same side or directly opposite to each other, the resulting tide is called spring tide; if they are perfectly perpendicular, the resulting tide is called neap tide [1]. The Chao Phraya River is located in Thailand's central region and has a flat plains area in the lower part, which is influenced by the tide. The tide characteristics of the Gulf of Thailand, which is affected by mixed tides, consist of two high and/or low tides on each tidal day. The height of each tide varies from day to day, resulting in changes in the water levels in the lower part of the Chao Phraya River, which ranges from the river mouth to Bang Sai, Ayutthaya province [2-3].

When the seawater level starts to fall from the highest level, it causes the water to continually flow into the sea with a profile of vertical velocity. The maximum and minimum flow rates in the river do not occur at the time when the water level has reached its highest or lowest points. The maximum flow rate into the sea is generated when the sea level sharply drops and approaches the lowest level, due to the extremely different upstream and downstream water levels [4-5].

The tide results in flow rate and sediment transport in two directions; where the river flows into the sea and where the seawater flows into the river. Consequently, the tidal affected area is where sediment accumulates that cause rivers to become shallow, blocking them from draining into the sea. Therefore, predicting flow rate and sediment transport in rivers is essential for water resources management, planning, navigation and environmental protections, including sediment problems in the factories' cooling systems.

Chen and Chiu (2002) proposed a quick and easy method to predict flow rate in a tidal river. The method is determined by the ratio between mean

velocity (V_{mean}) and maximum velocity (V_{max}) and considers the relationship between velocity and area. Additionally, Chen and Chui reported data from the Tanshui River based on tidal effects obtained using this method. Their results provided evidence that this efficient method is effective in predicting tide-influenced flow rates [6].

Recently, machine learning (ML) techniques have been used for many applications in water resources. These models can capture data's non-linearity, non-stationarity, noise, complexity and dynamism. These models can be categorized into four groups: classifiers and machine-learning approaches, fuzzy sets, evolutionary computation and wavelet conjunction models [7]. Comprehensive reviews of different ML techniques and their applications in water resources engineering can be found in [8-10].

Genetic programming (GP), a subset of ML, is an evolutionary approach. It is one of the most popular evolutionary computing techniques that use a Darwinian algorithm to solve problems [11]. This approach generates input-output relationships as explicit symbolic mathematical expressions. It is often regarded as a grey-box data-driven technique rather than as a black-box data-driven technique, such as Artificial Neural Networks (ANNs) or Support Vector Machines (SVMs) [10]. In recent decades, GP has been a successful tool in solving various kinds of engineering problems and has undergone early advancements, and its accuracy is higher than that of traditional programs [8, 12]. Moreover, GP can be applied in various water resource problems for estimation or prediction. Examples of such problems include rainfall runoff modelling [13-14], probabilistic flood forecasting [15-16], reservoir management [17], flood forecasting system prediction [18], water-level and storage-capacity curves [19], lake level prediction models [20], groundwater level forecast models [21], runoff forecasting [22], wave height forecasting [23-27], and suspended sediment modelling [28-33]. However, GP's utilization for tidal rivers has not yet been achieved.

Therefore, this research's aim is to develop simple models to predict flow rate and suspended sediment transport in the lower Chao Phraya River based on the tides' characteristics, which are rather complicated. The important hydraulic factors are determined and analysed to obtain their relationships.

2. THEORY

2.1 Relationship between water level and flow rate in the lower Chao Phraya River

For a uniform flow in an open channel, the discharge can be computed using Manning's principle as:

$$Q_0 = \frac{1}{n} A R^{\frac{2}{3}} S_0^{\frac{1}{2}} \quad (1)$$

where Q_0 is the discharge of uniform flow (m^3/s), n is the Manning's roughness coefficient ($s/m^{1/3}$), A is the cross-sectional area (m^2), R is the hydraulic radius of the river section (m), and S_0 is the bed slope (dimensionless).

However, in the case of non-uniform flow, the water surface slopes depend on flood hydrograph of upstream and tide from downstream. When the Manning's principle is

applied, the discharge could be expressed as:

$$Q_f = \frac{1}{n} A R^{\frac{2}{3}} S_f^{\frac{1}{2}} \quad (2)$$

where Q_f is the discharge of non-uniform flow (m^3/s), and S_f is the friction slope (dimensionless).

When the flood waves and tidal waves, moving through the river, the friction slope (S_f) does not consistently equal the water surface slope (S_w) or the bed slope (S_0). Therefore, a unique rating curve could not exist and the relationship between water level and flow rate in unsteady conditions leads to the loop pattern.

As mentioned earlier, the flow in the lower Chao Phraya River is influenced by tides. The study of this relationship between water level and flow rate was conducted at the Wat Bang Hua Suea station using field measurements during Oct. 2015 and May 2016. These months cover all tide seasons, including spring and neap tides [5].

2.2 Prediction by GP

GP is an evolutionary algorithm, which is a process inspired by the Darwinian theory of evolution. This approach offers results in the form of mathematical equations, involving various variables [11]. GP has many advantages: for example, it can be applied to areas where the interrelationships among the relevant variables are poorly understood or those where conventional mathematical analysis does not or cannot provide analytical solutions [34]. GP algorithms are often used as data fitting tools, thus making GP applications highly similar to those of other ML algorithms, such as artificial neural networks or support-vector machines [10]. GP's most unique and distinct feature, which differentiates it from other ML approaches, is its ability to test relationships and present the best ones. Practically, in stream-flow modelling and forecasting, evolutionary computation has scored higher in accuracy than other ML techniques such as artificial neural networks [7]. Many researchers have demonstrated evolutionary computations' capabilities [35-39].

The GP algorithm begins with random initial populations called potential solutions. During the training phase, the solutions that demonstrate high performance (during the fitness evaluation) survive to the next generation and are considered as parents to create offspring. Next, three evolutionary operators - namely, reproduction, crossover and mutation - are used to act on each individual solution to improve it to achieve a desired state [40]. Reproduction is the process of transferring the single best solution into the new population set without any change. Crossover refers to producing two new individuals by selecting a random subtree (i.e. function nodes) in each of the two parents and swapping the resultant subtrees, with the new individuals being the offspring. In the mutation, a subtree is randomly chosen and is removed and replaced by a randomly generated subtree [41]. A flow chart of the GP algorithm, which expresses the conceptual framework of the study, is shown in Figure 1.

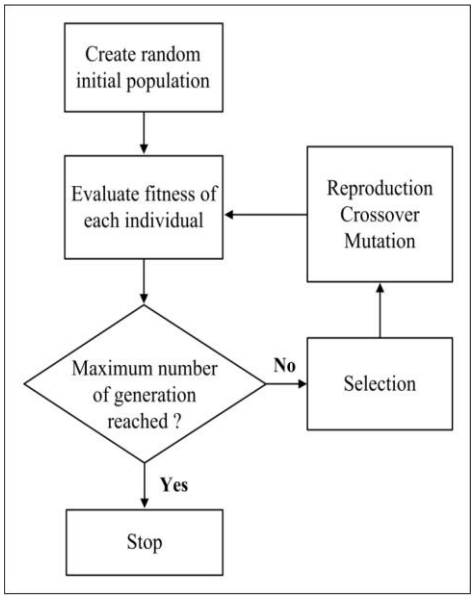

Figure 1 Simplified GP flowchart.

These looping processes are repeated until the optimal results are found or the maximum number of generations is reached. For testing, GP is used to determine various parameters, such as population size, crossover probability, mutation probability, reproduction probability, max tree depth, function set and generation numbers to find the optimal values for problem-solving. The probabilities of crossover and mutation are determined based on the application, but the probability of mutation is typically much smaller than that of crossover.

3. METHODOLOGY

3.1 Field data collection

Field data such as current velocity, sediment concentration, and flow depth were collected at the Wat Bang Hua Suea station between October and September 2019 (Figure 2). Water levels were collected at Bangkok Port, the Wat Bang Hua Suea and Chulachumklao Fort stations. The hydrographic department provided some hydrologic data. Bangkok Port's, the Wat Bang Hua Suea station's and Chulachomklao Fort station's distances from the mouth of the Chao Phraya River are 30 km, 14 km and 3 km, respectively. Instantaneous flow velocity was measured at any flow depth using a propeller current meter.

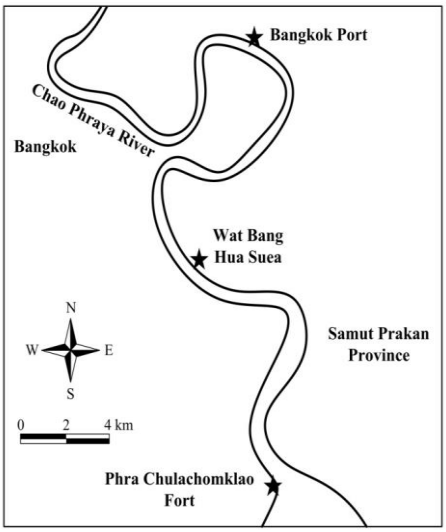

Figure 2 Locations of the field measurement.

The flow depths were measured using an echo sounder and a GPS, which were installed in a flat aluminum boat that travelled throughout the study area. The echo sounder works by pulsing ultrasonic wave signals transmitted from the sound wave transducer toward the river bed, from which the signal is reflected back to the sound wave sensor. Computation of the water depth value is based on the celerity of the sound wave and the travel time for the sound waves to reach the bottom and reflect back. The accuracy of these water level

measurements is within ±(1 cm + 0.1%) of water depth.

The flow velocity at the area's boundary was measured using the current meter (model FP211, Global Water). This tool features water flow velocity measurements ranging from 0.1 m/s to 6.1 m/s and a measurement accuracy within 0.03048 m/s. The front of the impeller was parallel to the direction of water flow. The measurements were taken when the water flowed, and the device's propeller was rotated around the horizontal axis for *N* rotations each time. The meter was installed at the downstream location to measure the flow velocities at different points in time during the test.

Suspended concentrations data were collected using the OBS-3A concentration meter, which uses the nephelometric method: It emits infrared light to the suspended particles in the water. Then, it uses infrared sensors to detect the scattered suspended particles. This tool's accuracy depends on the type of sludge: 2% for mud and 3.5% for sand.

3.2 Process of model development

To predict flow rate, flow depths are used as the input data. To predict sediment transport rate, the input data include flow depths, flow rates and water surface slopes. The data (current velocity, sediment concentration and depth) were measured in the lower Chao Phraya River between November 2015 and December 2016, which cover all the tide seasons [42].

GP testing and determination was achieved through the determination of parameters. Population size consists of the number of individuals involved in each generation; Crossover probability is the possibility of a crossover in a generation; Mutation probability is the possibility of mutation or creating a new generation in each individual; Reproduction probability is the possibility of individuals with high fitness to be selected for producing offspring of the next generation; Max tree depth is to avoid excessive growth of its individuals; function set is the set of calculated parameters consisted of arithmetic operations; and generation number is to determine the length of the genetic algorithm process.

By experimentally, the values of parameters used to set up GP in this study are summarized in Table 1. These parameters were set as constants, whereas the generation number was tested at 500, 1,000, 1,500, 2,500 and 3,000 to obtain the appropriate generation number.

After the appropriate generation number was obtained, it was fixed as a constant, and the next parameter was varied until it was found. To control the solution's complexity, only basic arithmetic operations were used as the members of the functional set. The root mean square error (RMSE) and correlation coefficient (*r*) values were used in the objective functions to train the GP model.

To create a GP-based model, the software GPdotNET v5.0 [40], an open-source computer program for running tree-based GP, was used. The data were split into two periods: the spring tide period and the neap tide period. The spring tide and neap tide data were each divided into 2 parts, one of which was used for the training

processes and the other of which was used for the testing processes.

Due to lacking of data of the mass influx and out flux of sediment in the study areas, the input data for the predictions contain the following elements.

Table 1. Parameters selected for GP set-up.

Parameter	Set-up value
Population size	500
Crossover probability	0.90
Mutation probability	0.05
Reproduction probability	0.20
Max tree depth	5.0
Function set	+, -, * and /
Generation number	500, 1,000, 1,500, 2,500 and 3,000

1) To predict the flow rate, the input data are the water levels at the Bangkok Port station and Chulachumklao Fort station. The data sets for developing GP models to predict discharge were 131. Those data sets were divided 70% (92 data sets) for the training process and 30% (39 data sets) for testing process. Mixed data of spring and neap tide were used.

2) To predict the sediment transport rate, the input data are the flow rates and flow depths at the Wat Bang Hua Suea station. The data sets for developing the GP model to predict sediment transport rate were 41. Those data sets were divided into two types, i.e., 25 data sets for spring tide and 16 data sets for neap tide. In addition, for spring tide, the data sets of 25 were divided 56% (14 data sets) for the training process and 44% (11 data sets) for the testing process. Those data sets for neap tide were divided 50% (8 data sets) for the training process and 50% (8 data sets) for the testing process

3.3 Criteria for evaluating model's performance

The correlation coefficient (r), RMSE and mean absolute error (MAE) were used in the model efficiency comparison. The correlation coefficient is used mainly to indicate accuracy because when the correlation coefficient is exactly 1, it indicates perfect accuracy. In contrast, when the correlation coefficient is close to 0, it indicates low accuracy. The performance evaluation criteria are given as follows:

$$r = \frac{\sum_{i=1}^{N}(X_i^{obs}-X_{mean}^{obs})(X_i^{pre}-X_{mean}^{pre})}{\sqrt{\sum_{i=1}^{N}(X_i^{obs}-X_{mean}^{obs})^2}\sqrt{\sum_{i=1}^{N}(X_i^{pre}-X_{mean}^{pre})^2}} \quad (3)$$

$$RMSE = \sqrt{\frac{\sum_{i=1}^{N}(X_i^{obs}-X_i^{pre})^2}{N}} \quad (4)$$

$$MAE = \frac{1}{N}\sum_{i=1}^{N}\left|X_i^{obs} - X_i^{pre}\right| \quad (5)$$

where X_i^{obs} is the observed data, X_i^{pre} is the predicted result, X_{mean}^{obs} is the mean observed value, X_{mean}^{pre} is the mean predicted value and N is the number of observations

4. RESULTS AND DISCUSSION

The flow rate and sediment transport rate field data were collected at Wat Bang Hua Suea station between 8 October and 21 November of 2019. There were 45 data sets, which were divided into 19 sets of spring tide data and 26 sets of neap tide data. The GP model was used to simulate and predict the flow rate and sediment transport rate, and the predictions were compared to the field data to evaluate their accuracy.

4.1 Hydrologic characteristics of flow influenced by tides

The relation between water levels (m) and flow rates (m^3/s) in the lower Chao Phraya River involves multiple loops, in which the water levels are associated with various flow rates depending on tidal levels. Accuracy in flow rate prediction is measured by the similarity between the rating curve and the data format.

The relationship between water levels and flow rates at Wat Bang Hua Suea station between October and November 2019 is indicated by loops, where the flows were in the range of -2,300 m^3/s to +2,000 m^3/s and the water levels were in the range of +0.10 m to +1.50 m (mean sea level), as shown in Figure3. The discharge during the ebb tide (falling tide) was positive while the discharge at the same stage during the flood tide (rising tide) was negative. Those discharges at the same stage were different in magnitudes. Moreover, the maximum and minimum flow rates in the river did not occur at the time when the water level reached its highest or lowest. Because seawater levels are influenced by tides, as shown in Figure4, the minimum flow rates occurred when the water level reached its peak and sea water flowed into the river and impeded the river from flowing into the sea. In contrast, the maximum flow rates occurred at the time when the water level reached its lowest, when the water in the river flowed into the sea.

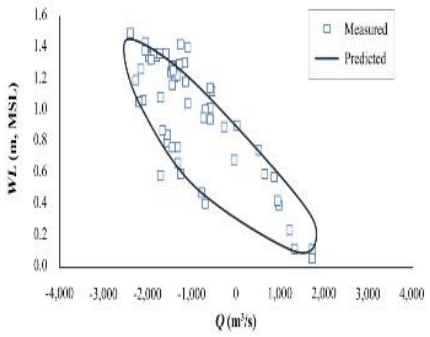

Figure 3 Water levels and flow rates at Wat Bang Hua Suea station (Oct. - Nov. 2019).

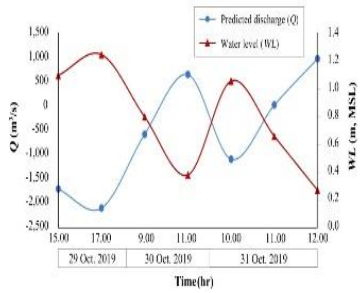

Figure 4 Water levels and flow rates at Wat Bang Hua Suea station (29 - 31 Oct. 2019)

The relationship between water levels and cross-sections was determined in the form of power regression using Chen and Chiu's method [6], which uses a constant ratio of the mean velocity (V_{mean}) and maximum velocity (V_{max}) of the considered river section. Within the range of data measured this study, the cross-sectional area of flow was determined and the flow rate at Wat Bang Hua Suea station can be expressed as follows:

$$Q = (0.6415\ V_{\max})\ A \quad (6)$$

where Q is flow rate (m^3/s), $V_{\max}$ is the maximum velocity (m/s), and A is the cross-sectional area (m^2)

4.2 Prediction of flow rate using GP model

Based on literature reviews, no previous study of river flow rates has used flow direction in a machine learning model. The lower Chao Phraya River's flow has two directions: (i) flow from upstream mentioned above, the flow rate has two directions (either upstream fresh water flows into the sea [flow rate is positive: +] or seawater flows backward into the river [flow rate is negative: -]), with flow rates of -3,000 m^3/s to +3,000 m^3/s. The trend of flow rate closely relates to the flow velocity during spring tide. During neap tide, the flow rate is unidirectional: The seawater flows into the river, meaning the flow rate out to the sea (+) and (ii) flow from the sea into river (-). This study's flow rate prediction is based on a mathematical model using GP principles for correlation analysis, which is used to convert data into mathematical equations.

Using data sets of 131 for field survey during November 2015 and March 2016. The developed equation containing flow rates (m^3/s) and water levels (m) covers all tide seasons, including spring tide and neap tide, and can be expressed as follows:

$$Q = f_1\ (WL_1, WL_2, \text{flow direction}) \quad (7)$$

where Q is the predicted flow rate (m^3/s), WL_1 is the water level at Bangkok port station (m), WL_2 is the water level at Chulachumklao Fort (m) and flow direction is represented by a positive or negative.

The predicted flow rate results using GP and the looped rating curve were compared with flows in the field measurement. As is negative. The neap tide period has a smaller flow rate range than the spring tide period, with flow rates ranging from -2,500 m^3/s to +2,050 m^3/s.

The flow rate forecasting performance of this method was satisfactory. The relations between observed and predicted flow rates during the spring and neap tides are shown in Figures 5 and 6, respectively.

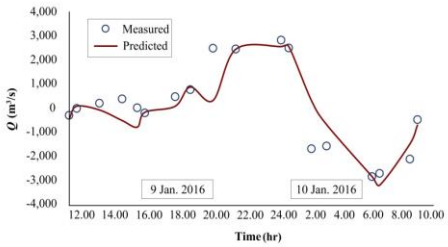

Figure 5 GP model flow rate prediction during spring tide.

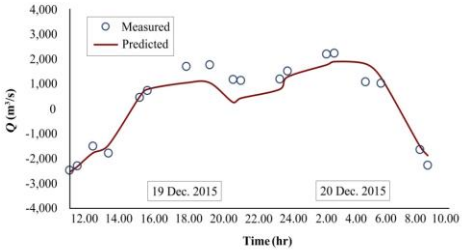

Figure 6 GP model flow rate prediction during neap tide.

The GP model (Eq. 7) demonstrated satisfactory performance with a correlation coefficient (r) of 0.887, an RMSE of 710.491 m^3/s and an MAE of 539.885 m^3/s for the training processes. For the testing processes, those values were 0.943, 818.988 m^3/s and 665.242 m^3/s, respectively.

4.3 Prediction of sediment transport rate using GP model

Spring tide and neap tide influence the behaviour of flow rates and sediment transport rates in the lower Chao Phraya River. In the case of spring tide, flow rate and sediment transport rate have two directions, while the neap tide features a unidirectional flow, where the seawater flows into the river. Moreover, the estimated sediment transport rate closely correlates with the flow rate.

The sediment transport rate relationships may be classified into three forms: (i) the relationship between the sediment transport rate and the flow rate, (ii) the relationships between the sediment transport rate and depth and between flow rate and depth, and (iii) the relationship among sediment transport rate, flow rate and water surface slope. These relationships can be illustrated using the linear and GP equations by further analysing the flow depth and surface slope data. As a result of the water level change caused by tidal influence on the river, water depth change causes changes in the flow and sediment transport rates. Additionally, the difference between the upstream and downstream water levels determines the water surface slope and the flow direction caused by the tide's influence. All of these factors influence the sediment transport rate. The hydraulics data indicated that sediment transport rate changes in the tidal river are influenced by spring and neap tides.

The developed equation can be expressed either functions of flow rates and flow depth or flow rate and water surface slope can be expressed as follows:

$$q_s = f_2\,(Q, y, \text{flow direction}) \quad (8)$$

$$q_s = f_3\,(Q, S_w, \text{flow direction}) \quad (9)$$

where q_s is the nearshore sediment transport rate ($g/m^2/s$), Q is the flow rate (m^3/s), y is the flow depth (m), S_w is the water surface slope, and flow direction is represented by a positive or negative.

Prediction results obtained from Eqs. (8) and (9) were compared with field measurements. Then, statistical indexes were used to compare the predicted results to select the most optimal model. It was found that the GP model using Eq. (8) based on the flow

rate and flow depth variables predicted the sediment transport rate with the value closest to the observed data in both spring and neap tides. These results had high correlation coefficient (*r*) values in both the training processes and the testing processes. It was found that the model's prediction results reflected satisfactory performance and were highly accurate in both the spring tide period and neap tide period, as shown in Figures 7 and 8.

These results had high correlation coefficient (*r*) values in both the training processes and the testing processes. It was found that the model's prediction results reflected satisfactory performance and were highly accurate in both the spring tide period and neap tide period. However, it is noted that the model is incapable of predicting the sudden increase in the sediment transport rate.

The GP model using Eq. (8) demonstrated satisfactory performance during the spring tide period with a correlation coefficient (*r*) of 0.960, an RMSE of 0.054 g/m^2/s and an MAE of 0.027 g/m^2/s for the training processes. For the testing processes, the values were 0.728, 0.147 g/m^2/s and 0.113 g/m^2/s, respectively. During the neap tide period, the GP model shows a correlation coefficient (*r*) value of 0.969, an RMSE of 0.026 g/m^2/s and an MAE of 0.017 g/m^2/s for the training processes. Whereas the same values are 0.645, 0.060 g/m^2/s and 0.045 g/m^2/s, respectively, for the testing processes. For this case, the value of *r* is quite low because of the limited amount of field data and the nature of variation of parameters involved in the tidal phenomena.

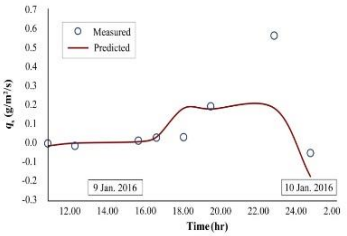

Figure 7 Spring tide period sediment transport rate prediction

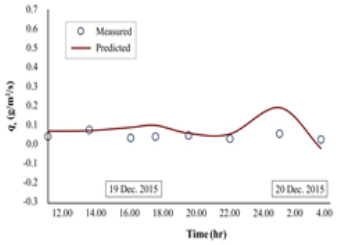

Figure 8 Neap tide period sediment transport rate prediction.

The results demonstrate that the proposed GP model with high *r* values and low RMSE and MAE values can predict the flow and nearshore sediment transport rates with satisfactory performance. The proposed GP model identified the flow direction as an important parameter affecting flow and sediment transport rates in the studied tidal river. Additionally, it is clear that this GP model can be used for practical flow and nearshore sediment transport rate applications in this tidal river.

5. CONCLUSIONS

The flow direction, which was used in the proposed GP model, was shown to be an important parameter affecting flow and nearshore sediment transport rates in the studied tidal river. The prediction results show accurate

performance, correlation coefficient (*r*) values greater than 0.88 for training and testing processes. Regarding the sediment transport rates, the GP model equation used to predict these rates demonstrated good performance with RMSE and MAE values close to those of the observed data. The spring tide flow and sediment transport rates determined by the GP model are more accurate than those for the neap tide period. This difference is because during spring tide, there is a greater water level change than the change during neap tide. For this reason, water level changes during the spring tide period had a greater influence on the flow rate and velocity than the changes during the neap tide period. Given that compared to for the spring tide period, the predicted flow rate was a little bit more accurate for the neap tide period, the predicted sediment transport rate for the neap tide was a little bit more accurate as well. Hence, this model can be applied to effectively predict the flow rate and nearshore sediment load in the lower Chao Phraya River.

6. ACKNOWLEDGMENT

The authors would like to thank researchers of WAREE, KMUTT for their assistance in field measurement. Partly financial support from Electricity Generating Authority of Thailand (EGAT) is also appreciated.

7. REFERENCES

[1] Hicks S.D. Understanding tides. NOAA National Ocean Service. Silver Spring. MD. USA. 2006. DOI: 10.25607/OBP-157.

[2] Maghrebi M.F. and Givehchi M. Discharge estimation in a tidal river with partially reverse flow. Journal of Waterway, Port, Coastal and Ocean Engineering. 2010; 136(5): 266-274. DOI:10.1061/(ASCE)WW.1943-5460.0000049.

[3] Chinnarasri C. and Kemden N. Discharge estimation of a tidal river with reverse flow: Case of the Chao Phraya River, Thailand. Journal of Hydrologic Engineering. 2016; 21(4). DOI:10.1061/(ASCE)HE.1943-5584.0001323.

[4] Voulgaris G. and Trowbridge J.H. Evaluation of the Acoustic Doppler Velocimeter (ADV) for turbulence Measurements. Journal of Atmospheric and Oceanic Technology. 1998; 15(1): 272-289. DOI:10.1175/15200426(1998)015<0272:EOTADV>2.0.O;2.

[5] Chinnarasri C., Phothiwijit K. and Apipattanavis S. A study of flow characteristics in the lower Chao Phraya River using Acoustic Doppler Velocity Technology, Engineering Journal of Research and Development. 2017; 40(2): 217-235.

[6] Chen Y.C., and Chiu C.L. An efficient method of discharge measurement in tidal streams. Journal of Hydrology. 2002; 265(1-4): 212-224. DOI:10.1016/S0022-1694(02)00100- 2.

[7] Yaseen Z.M., El-shafie A., Jaafar O., et al. Artificial intelligence based models for stream-flow forecasting: 2000-2015. J. Hydrol. 2015; 530: 829-844. DOI:10.1016/j.jhydrol.2015.10.038.

[8] Danandeh Mehr A., Nourani V., Kahya E., et al. Genetic

programming in water resources engineering: a state-of-the-art review. Journal of Hydrology. 2018; 566:643-667. DOI:10.1016/j.jhydrol.2018.09.043.

[9] Govindaraju R.S. Artificial neural networks in hydrology II: Hydrologic applications. Journal of Hydrologic Engineering. 2000; 5: 124-137. DOI:10.1061/(ASCE)1084-0699(2000)5:2(124).

[10] Herath H.M.V.V., Chadalawada J., and Babovic V. Genetic programming for hydrological applications: to model or to forecast that is the question. Journal of Hydroinformatics. 2021; DOI:10.2166/hydro.2021.179.

[11] Koza J.R. Genetic Programming: on the programming of computers by means of natural selection. MIT Press. Cambridge MA. 1992.

[12] Fallah-Mehdipour E. and Haddad O.B. Application of genetic programming in hydrology. In: Handbook of Genetic Programming Applications (A. H. Gandomi, A. H. Alavi and C. Ryan, eds.) Springer. 2015: 59-70.

[13] Babovic V. and Keijzer M. Rainfall runoff modelling based on genetic programming, Hydrology Research. 2002; 33(5): 331-346. DOI:10.2166/ nh.2002.0012.

[14] Havlicek V., Hanel M., Maca P., et al. Incorporating basic hydrological concepts into genetic programming for rainfall-runoff forecasting. Computing. 2013; 95(1): 363-380. DOI:10.1007/s00607-013-0298-0.

[15] Mediero L., Garrote L. and Chavez- Jimenez A. Improving probabilistic flood forecasting through a data assimilation scheme based on genetic programming, Nat. Hazards Earth Syst. Sci. 2012; 12: 3719-3732. DOI:10.5194/nhess-12-3719-2012, 2012.

[16] Ji H., Songlin W., Qinglin W., et al. Douhe reservoir flood forecasting model based on data mining technology. Procedia Environmental Sciences. 2012; 12: 93-98. DOI: 10.1016/j.proenv.2012.01.252

[17] Fallah-Mehdipour E., Bozorg Haddad O.B., and Marino M.A. Developing reservoir operational decision rule by Genetic Programming. Journal of Hydroinformatics. 2013; 15(1): 103-119. DOI: 10.2166/hydro.2012.140.

[18] Watanabe N., Fukami K., Imamura H., et al. Flood forecasting technology with radar-derived rainfall data using genetic programming, International Joint Conference on Neural Networks. Atlanta GA, USA, 14-19 June 2009: pp. 3311-3318.

[19] Hongyan L., Shan J., and Xinhua B. Application of genetic programming to identifying water-level and storage-capacity curve of the Xingxingshao Reservoir, Asia-Pacific Power and Energy Engineering Conference (APPEEC 2009).

Wuhan, China, 27-31 March 2009: pp. 9-11.

[20] Aytek A., Kisi O., and Guven A. A genetic programming technique for lake level modeling. Hydrology Research. 2014; 45(4-5): 529–539. DOI: 10.2166/ nh.2013.069.

[21] Kasiviswanathan K.S., Saravanan S., Balamurugan M., et al. Genetic Programming based monthly groundwater level forecast models with uncertainty quantification. Modeling Earth Systems and Environment. 2016; 2(27): 1-11. DOI: 10.1007/s40808-016- 0083-0.

[22] Khu S.T., Liong S.Y., Babovic V., et al. Genetic programming and its application in real-time runoff forecasting. Journal of the American Water Resources Association. 2001; 37(2): 439–451. DOI: 10.1111/ j.1752-1688.2001.tb00980.x.

[23] Kalra R. and Deo M.C. Genetic programming for retrieving missing information in wave records along the west coast of India. Applied Ocean Research. 2007; 29(3): 99-111. DOI: 10.1016/j.apor.2007.11.002.

[24] Ustoorikar K. and Deo M.C. Filling up gaps in wave data with genetic programming. Marine Structures. 2008; 21: 177-195. DOI: 10.1016/ j.marstruc.2007.12.001.

[25] Gaur S. and Deo M.C. Real-time wave forecasting using genetic programming. Ocean Engineering. 2008; 35(11-12): 1166-1172. DOI: 10.1016/j.oceaneng. 2008.04.007.

[26] Londhe S.N. Soft computing approach for real-time estimation for missing wave heights. Ocean Engineering. 2008; 35: 1080-1089. DOI:10.1016/j.oceaneng.2008.05 .003.

[27] Roy C., Motamedi S., Hashim R., et al. A comparative study for estimation of wave height using traditional and hybrid soft-computing methods. Environmental Earth Sciences. 2016; 75(7): 590. DOI: 10.1007/s12665-015- 5221-x.

[28] Aytek A. and Kisi Ö. A genetic programming approach to suspended sediment modeling. Journal of Hydrology. 2008; 351(3–4): 288–298. DOI: 10.1016/j.jhydrol.2007.12.005.

[29] Rezapour O.M., Shui L.T., and Dehghani A.A. Review of genetic algorithm model for suspended sediment estimation. Aust. J. Basic Appl. Sci. 2010; 4(8): 3354-3359.

[30] Guven A. and Kisi O. Estimation of suspended sediment yield in natural rivers using machine-coded linear genetic programming. Water Resources Management. 2011; 25(2): 691-704. DOI: 10.1007/s11269-010-9721-x.

[31] Kisi O. and Shiri J. River suspended sediment estimation by climatic variables implication: Comparative study among soft computing techniques. Comput. Geosci. 2012; 43: 73-82. DOI:10.1016/j.cageo.2012.02.00 7.

[32] Danandeh Mehr A. and Sorman A.U. Streamflow and sediment load prediction using linear genetic programming. Uludag University Journal of The Faculty of Engineering. 2018; 23(2): 323-332. DOI: 10.17482/UUmfd.352833.

[33] Idrees M.B., Jehanzaib M., Kim D., et al. Comprehensive evaluation of machine learning models for suspended sediment load inflow prediction in a reservoir. Stochastic Environmental Research and Risk Assessment. 2021; 35: 1805-1823. DOI: 10.1007/s00477-021-01982-6.

[34] Banzhaf W., Nordin P., Keller R. E., et al. Genetic programming: An introduction on the automatic evolution of computer programs and its applications. Morgan Kaufmann Publishers, Inc., San Francisco, California. 1998.

[35] Friedel M.J. A data-driven approach for modeling post-fire debris-flow volumes and their uncertainty. Environ. Model. Softw. 2011; 26: 1583–1598. DOI: 10.1016/j.envsoft.2011.07.014.

[36] Dumedah G. Toward essential union between evolutionary strategy and data assimilation for model diagnostics: An application for reducing the search space of optimization problems using hydrologic genome map. Environ. Model. Softw. 2014; 69: 342–352. DOI:10.1016/j.envsoft.2014.09.025.

[37] Maier H.R., Kapelan Z., Kasprzyk J., et al. Evolutionary algorithms and other metaheuristics in water resources: current status, research challenges and future directions. Environ. Model. Softw. 2014; 62: 271–299. DOI: 10.1016/j.envsoft.2014.09.013.

[38] Tran H.D., Muttil N., and Perera B.J.C. Selection of significant input variables for time series forecasting. Environ. Model. Softw. 2015; 64: 156–163. DOI: 10.1016/j.envsoft.2014.11.018.

[39] Zimmer A., Schmidt A., Ostfeld A., et al. Evolutionary algorithm enhancement for model predictive control and real-time decision support. Environ. Model. Softw. 2015; 69:330–341.DOI: 10.1016/j.envsoft.2015.03.005.

[40] Hrnjica B. and Danandeh Mehr A. Optimized Genetic Programming Applications: Emerging Research and Opportunities. IGI Global, Hershey, PA. 2019: p. 310.

[41] Danandeh Mehr A. and Safari M.J.S. Genetic programming for streamflow forecasting: a concise review of univariate models with a case study. Advances in Streamflow Forecasting. 2021; 193-214: DOI: 10.1016/B978-0-12-820673-7.00007-X.

[42] Thammapraserddee N. and Chinnarasri C. Behavior of suspended sediment at the lower Chao Phraya River. Engineering Journal of Research and Development. 2019; 30(3): 7-29.